The Emergent Influence of Anthropogenic Warming on Global Crop Yields

Major Classification: Physical Sciences

Minor Classification: Social Sciences

Corresponding Author:
Frances C. Moore
Department of Environmental Science and Policy
2140 Wickson Hall
One Shields Ave
Davis, CA 95616 USA

fmoore@ucdavis.edu
617-233-3380

Abstract

A large literature on "detection and attribution" has now demonstrated the influence of anthropogenic greenhouse gas emissions on a range of physical climate variables. Social and economic outcomes are known to be sensitive to climate change, but directly connecting observed changes to anthropogenic forcing is challenging. Here I estimate the effect of anthropogenic warming on global crop yield trends, showing it is characterized by a general slowing of wheat and maize yields and an acceleration of rice yields in cooler regions. This global, multi-crop signal emerged in the early 2010s from the noise of internal climate variability, uncertainty in the yield response to temperature, and other sources of yield variability. The anthropogenic warming signal is apparent in the observed pattern of yield growth across countries and crops. The net effect has been negative, reducing annual calorie production from these crops by 5.3% on average over the 2008-2017 period, though simple calculations suggest this has likely been fully compensated, at a global level, by gains from CO_2 fertilization. This therefore provides early evidence that anthropogenic warming is already having a discernable effect on socio-economic systems at the global scale.

Significance Statement

Socio-economic systems are thought to be sensitive to climate change, but directly detecting climate change effects is challenging. This paper shows that the signal of anthropogenic warming on agriculture emerged globally in the early 2010s and can now be detected with high confidence. The anthropogenic warming effect involves acceleration of rice yields in temperate countries and a deceleration of wheat and maize yields in many areas. The estimated net effect on annual calorie production from wheat, rice, and maize each year of is a reduction of 5.3%, enough to feed 290 million. This provides early evidence that anthropogenic warming is already having a discernable effect on socio-economic systems at the global scale.

Main Text

Changes in many physical climate variables, including atmospheric temperature (1, 2), ocean heat content (3), streamflow (3), and the distribution and intensity of rainfall events (4–6), have now been detected and formally attributed to greenhouse gas emissions. Attribution of observed changes requires identifying a spatio-temporal pattern (or 'fingerprint') associated with anthropogenic climate change, demonstrating this pattern in observations, and showing that this pattern could not have arisen in the absence of anthropogenic emissions.

Many social and economic outcomes, ranging from aggregate economic productivity (7) to conflict (8) to human health (9), are thought to be sensitive to climate change. But attribution of observed changes to greenhouse gas emissions is extremely challenging: climate and weather explain only a small fraction of spatial and temporal variance in most outcomes; the response to climate drivers may be heterogeneous, non-linear, and poorly understood; observations at large geographic scales over sufficiently long time spans may be unavailable or unreliable; and the influence of many other drivers, some of which may be unobserved, confounds the climate change signal (10, 11). Only a tiny fraction of studies assessed by the IPCC dealt with observed impacts in human and managed systems, and confidence in the attribution of impacts to anthropogenic climate change ranged from very low to medium (11).

Agriculture is an economic sector that is both highly exposed and sensitive to climate change. A large literature has now established that yields respond to temperature fluctuations and that future warming will likely negatively affect agricultural productivity (12–16). Nevertheless, the dominant feature of yields in the second half of the 20th century has been a large and steady increase associated with higher input use and large technological improvements (Supplementary Figure 1a). A stagnation of yield growth since the 1990s, particularly for wheat, has been widely documented (17–19), with a variety of possible explanations advanced including slowing of R&D spending due to low prices, restrictions on fertilizer use in Europe, or biophysical limits to yield (20).

Supplementary Figure 1b shows the distribution of changes in yield growth by crop and climate region between 1961-1980 and 1998-2017. The slowing of yield growth, particularly for wheat, has been concentrated in the warmest part of its growing area, while both rice and maize have seen smaller gains in the very coldest parts of their range. There are multiple pathways through which hot temperatures reduce yields, with several papers pointing to the important role of higher vapor-pressure deficit in driving evapo-transpiration that lowers available soil moisture late in the growing season (12, 21, 22).

Other mechanisms include direct damage during the reproductive phase of the crop life-cycle and accelerated senescence that limits grain filling (23, 24). Given that growing season warming trends over growing areas have been documented in many locations (25), the patterns shown in Supplementary Figure 1b could be consistent with an emerging signal of anthropogenic warming on global yield growth.

However, connecting anthropogenic warming with the global pattern of changes in crop yield growth requires several steps. The observation that there has been warming over many growing areas during the growing season is not evidence that agriculture has been exposed to anthropogenic warming without assessing the likelihood of this warming occurring in the absence of greenhouse gas emissions. Natural variability at the subnational scale, even on multi-decadal time spans, is fairly large (26, 27) meaning counterfactual simulations of natural variability without greenhouse gas emissions are required to formally attribute observed warming to anthropogenic emissions. Although emergence of the anthropogenic signal in surface temperatures is well-established (1, 28), attribution of growing season temperature trends to human activity has only previously been done for western and northern Europe (29).

Second, the attribution of observed yield trends to warming requires ruling out other potential drivers. This is particularly difficult in most human and managed systems because climate fluctuations typically explain only a very small fraction of variation in outcomes. Although some previous work has estimated the effect of observed weather trends on crop yields using both empirical and process-based crop models (25, 30–36), this literature has not connected estimated impacts to observed yield trends nor attempted to distinguish the role of warming from other drivers of yield, with the limited exception of French wheat yields (37). Detection of an anthropogenic signal requires establishing the likelihood of observations in the absence of greenhouse gas emissions and this has not been done for any human or managed system at the global scale.

This paper uses two large ensembles of the CESM over the 20th century (LENS); one using all human and natural forcing (40 members, referred to as the "historical ensemble" in this paper) and one using all human and natural forcing except greenhouse gas emissions, which are fixed at 1920 levels (20 members, referred to as the "counterfactual ensemble" in this paper) (38) to characterize the effect of greenhouse gas emissions on growing season temperature. These ensembles are combined with yield-temperature response functions for wheat, rice, and maize derived both from an empirical crop model and an ensemble of gridded process-based crop models (39, 40) to estimate the effect of historic warming on yield growth. The natural variability in historical temperatures, represented in the climate

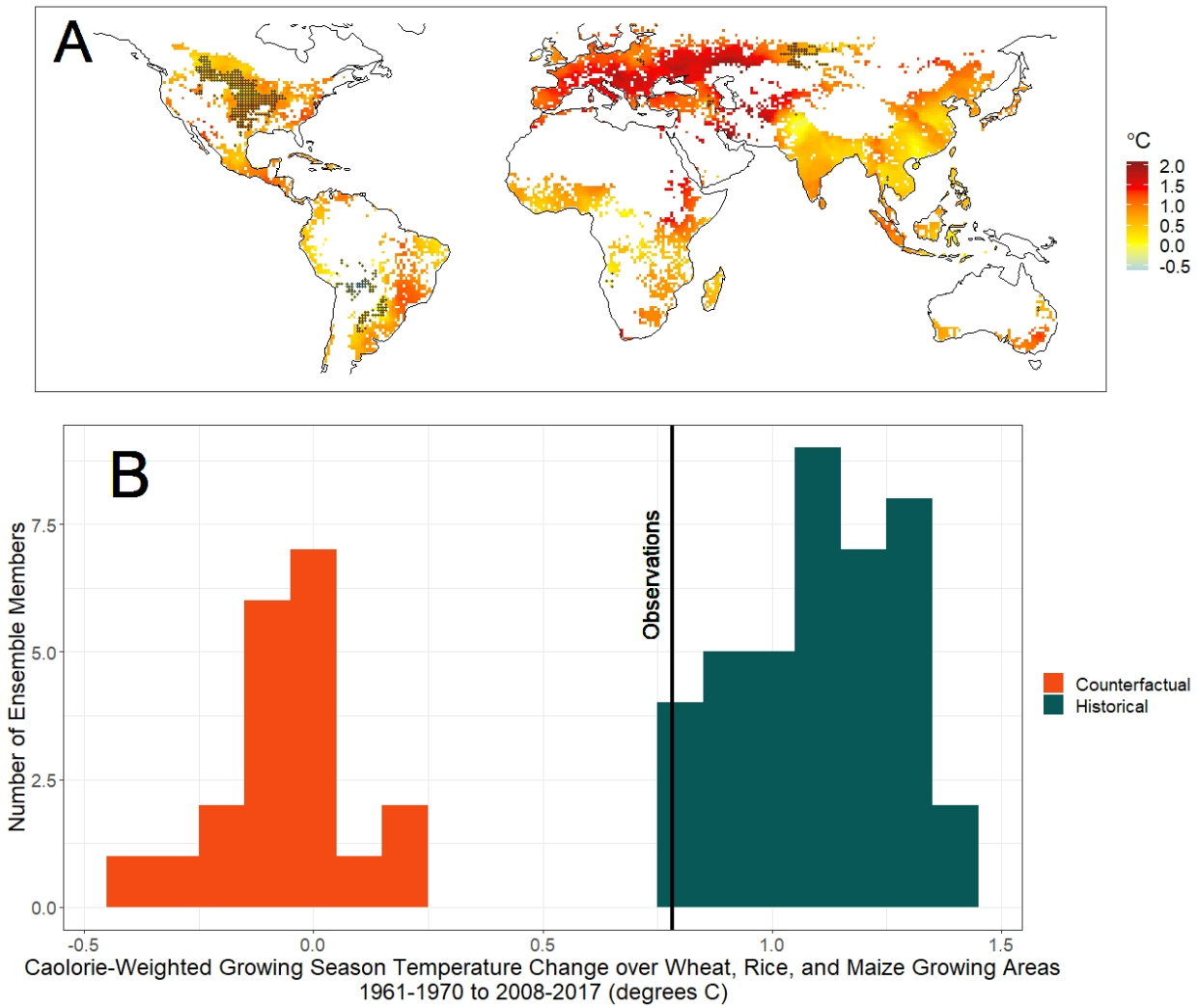

Figure One: Detection of anthropogenic warming signal over global crop areas and seasons. a) Observed change in growing season temperature over wheat, rice and maize growing areas (grid cells with >50 Ha combined in 2000 (41)) between 1961-1970 and 2008-2017 (42). Growing-season trends for the three crops are a calorie-weighted average of production for each grid cell. Black dots indicate areas where the observed warming is less than the 95th percentile of warming over the same period observed in the counterfactual climate model ensemble, which omits forcing from greenhouse gas emissions since 1920. b) Weighted average of growing season temperature trends for wheat, rice, and maize, aggregated based on calorie production in 2000, from the LENS ensemble under historical (40 members, blue) and counterfactual forcing (20 members, orange). Also shown is the observed warming of 0.8°C

model ensembles, is convolved with uncertainty in the yield response to temperature and variability resulting from non-temperature drivers of yield, to give distributions of possible yield trajectories between 1961 and 2017 for 287 crop-country combinations. Aggregating into a one-dimensional index designed to maximize power to detect the climate change signal, I show two main things: Firstly, the estimated effect of anthropogenic warming on global yield growth is large relative to noise from internal climate variability, uncertainty in the yield response to temperature, and variation from non-temperature drivers of yield (i.e. signal emergence). Secondly, the observed pattern of yield growth across countries and crops is consistent with the influence of anthropogenic warming (i.e. signal detection). I then discuss the degree to which this detected signal can or cannot be confidently attributed to anthropogenic warming (additional details Methods, Supplementary Figure 2).

Figure 1 demonstrates that an anthropogenic warming signal has emerged over crop growing areas during the growing season. Figure 1a shows observed growing-season warming over wheat, rice, and maize growing areas between 1961-1970 and 2008-2017, the period for which global yield data exist, and a comparison to the distribution of warming trends from the counterfactual climate model ensemble. Observed growing-season warming almost everywhere cannot be explained without greenhouse gas emissions, a notable exception being the "warming hole" over the US Midwest previously documented (43, 44). Aggregating to the global level on a calorie-production-weighted basis, the observed warming of 0.8°C is consistent with the distribution under historical forcing but not under the counterfactual forcing. The probability that greenhouse gas emissions were necessary and sufficient to cause the growing-season warming trend over growing areas observed during this time period (PNS, a measure of the separation of the historical and counterfactual distributions (45, 46)), is greater than 0.9999.

Supplementary Figure 3 shows the observed growing season rainfall changes over the 1961-1970 to 2008-2017 period, also compared to the counterfactual forcing distribution. Unlike temperature, an anthropogenic signal in growing-season rainfall has not emerged over many areas over this time period. This is not surprising given the substantial internal variability in decadal rainfall patterns (27, 47). The detection exercise therefore focuses only on the warming effect of anthropogenic greenhouse gas emissions, controlling for the effect of observed changes in rainfall on crop yields, but not attempting to attribute those changes to anthropogenic influence (Supplementary Figure 2), though this is relaxed in a supplementary analysis that includes the effect of internal variability in growing season rainfall.

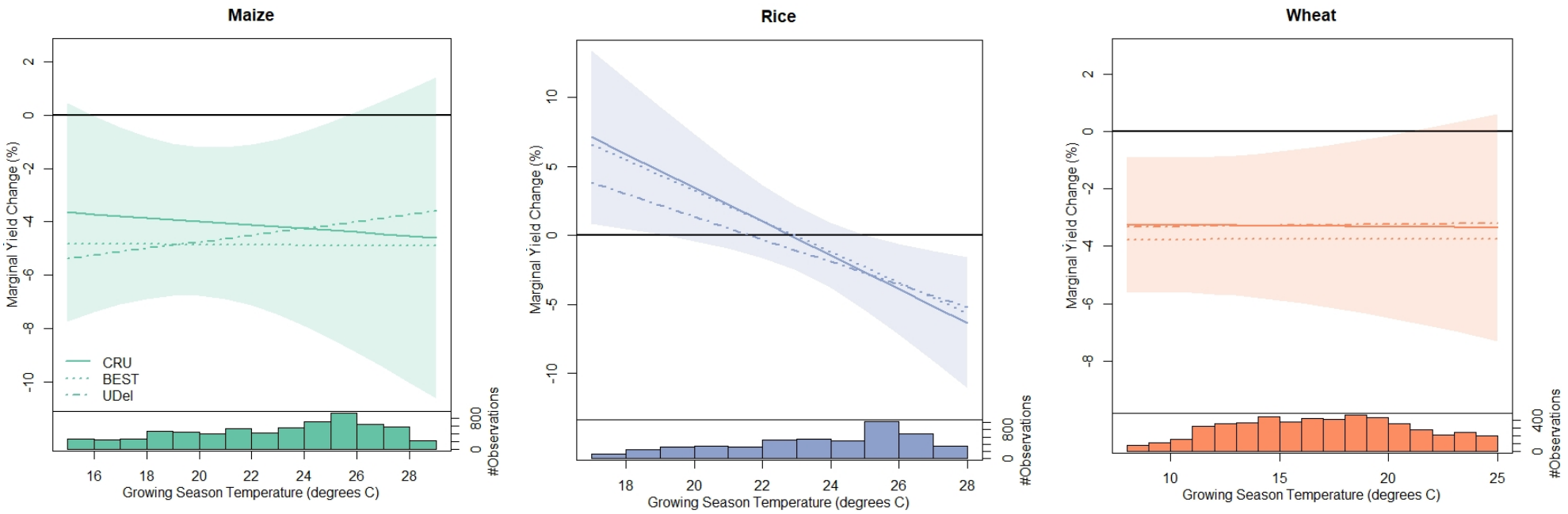

Figure Two: Sensitivity of Crop Yields to Warming. Effect of 1°C warming at different growing-season temperatures (marginal effect) estimated from the empirical crop model using three datasets for observed temperatures (Methods) for maize, rice and wheat. Values greater than zero indicate warming has a positive effect and less than zero indicate a negative effect. Shaded areas show the 95% confidence intervals using the CRU dataset, with two-way clustering of residuals at the region * crop level and the year * region level. Histograms show the distribution of observed growing season temperatures. Geographic regions used for clustering are given in Methods.

Figure 2 show the sensitivity of crops to warming estimated in the empirical crop model. The model specification follows Lobell et al. (25) and includes country-crop fixed-effects (dummy variables), crop-year fixed-effects, and country-crop quadratic time trends that control for all time-invariant differences and smoothly varying effects on yield, as well as controls for seasonal rainfall. The model finds largely linear, negative effects of warming over the range of maize and wheat areas, as well as non-linear effects on rice yields, which benefits from warming in the cooler part of its range. The estimated response is also robust to alternate observed temperature datasets (shown as dotted and dashed lines in Figure 2). Although the constant marginal effect of warming on wheat and maize yields across warm and cold areas may be surprising, this is not dissimilar from previous results. For example, in a meta-analysis of yield impact studies from mostly process-based crop models, both Challinor et al. (48) and Moore et al. (49), using different statistical methods, find little evidence for differing marginal effects on wheat and maize across warm and cool growing areas. Using a similar empirical crop model to that shown here, Lobell et al. (25) also do not find evidence for systematic differences in the marginal effects of warming across different regions.

Supplementary Figure 4 shows a systematic comparison between the marginal effects of warming estimated from the empirical model and from the Global Gridded Crop Model Inter-comparison (GGCMI) Phase 2 process-based crop model ensemble (39, 40). The process-based crop models do show on average more heterogeneous warming effects across baseline climates, including positive effects of warming on wheat and maize yields in some areas. But variation across the crop models is very large; uncertainty ranges from the empirical model and process-based crop model ensemble are non-overlapping for only 30 crop-country combinations, representing ~6% of crop area in the study. For 13 of these cases (12 wheat and 1 maize, mostly in cooler areas) the process-based estimate is more positive than the empirical estimate, while for 17 cases (3 wheat and 14 rice, mostly in warmer areas) the empirical estimate is more positive.

Supplementary Figure 5 shows the estimated response to growing season precipitation. The effect is in the expected direction, with higher rainfall most beneficial in dry regions, providing declining benefits in wetter areas. The estimates are empirically fairly small compared to temperature: an increase of 10% in growing season rainfall, approximately double the mean observed absolute change in growing season precipitation since 1961, increases yields of maize and wheat by 1.5%, 0.4%, and has essentially no effect on rice yields. Except for maize, these are not statistically distinguishable from zero. These results follow previous findings in the literature, which has generally found trends in growing season rainfall to

be not clearly distinguishable from zero and the empirical effects on crop yields to be small (21, 25, 50, 51).

In addition to controlling for observed growing-season rainfall, the empirical crop model controls for non-temperature drivers of yield through both country and crop-specific quadratic time trends that control for smooth, non-linear drivers of yield, and crop-year fixed-effects (dummy variables) that flexibly capture all crop-specific global yield shocks (Methods). Together, these account for the genetic progress in crop varieties, smooth increases in input use, and all other smoothly-varying or common global factors that might affect yields. Evidence for the effect of climate change is identified using deviations away from these time trends (additional discussion in Methods)

Figure 3a shows the change in yield between the first and last ten years of the sample (1961-1970 and 2008-2017) not explained by either the country-crop time trends or the crop-year fixed effects. The observed pattern shows a substantial slowing of yield growth, particularly for wheat and maize in parts of Africa and South America, as well as accelerations of rice yield growth in temperate parts of Europe, South America, and southern Africa, which have only small growing areas compared to the major rice producers in Asia. Figure 3a also shows the same measure of crop yield changes derived from two 1000-member yield ensembles generated by connecting the historical forcing and counterfactual forcing climate model ensembles with the empirical yield model. These yield simulations account for four sources of variation: 1) internal climate variability (via the climate model ensemble), 2) uncertainty in the yield response to temperature change (by sampling the parameters of the yield model), 3) variance in non-temperature factors in the empirical yield model (by sampling other parameter values in the empirical model), and 4) variation in yield unexplained by the empirical model (by sampling the residual distribution of the yield model).

The historical forcing ensemble captures important characteristics of the observed pattern of yield growth since 1960, particularly slowing wheat yield growth over much of Africa and Europe and accelerating rice yields in cooler growing regions. These patterns are not apparent in the counterfactual forcing ensemble (Figure 3a). Figure 3b shows the correlation between observed yield changes and the ensemble means, confirming that simulations using historical forcing capture observed patterns across crops and countries ($p<0.0001$), while counterfactual simulations excluding greenhouse gas forcing do not ($p=0.48$). Note that while there is a positive association between observed and simulated yield trajectories under the historical forcing ensemble, there is considerable variance in the observations not

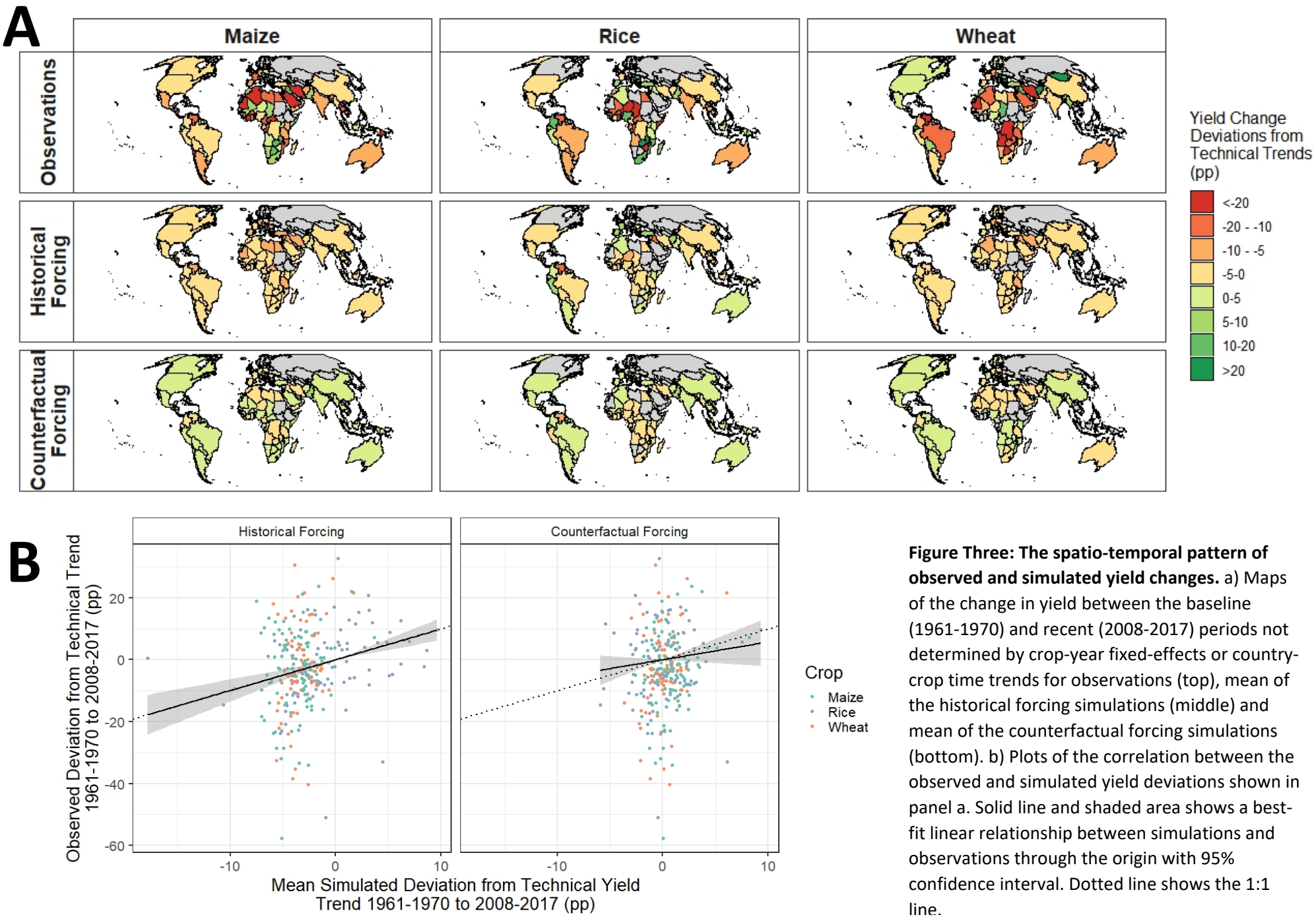

Figure Three: The spatio-temporal pattern of observed and simulated yield changes. a) Maps of the change in yield between the baseline (1961-1970) and recent (2008-2017) periods not determined by crop-year fixed-effects or country-crop time trends for observations (top), mean of the historical forcing simulations (middle) and mean of the counterfactual forcing simulations (bottom). b) Plots of the correlation between the observed and simulated yield deviations shown in panel a. Solid line and shaded area shows a best-fit linear relationship between simulations and observations through the origin with 95% confidence interval. Dotted line shows the 1:1 line.

captured by the yield model. In particular, the observations exhibit much larger yield declines in some areas across all three crops than can be explained with the estimated empirical temperature response.

While patterns from the ensemble means are suggestive, the variance resulting from convolving the range in the CESM ensemble with uncertainty in the parameters of the yield model is substantial. For any one crop-country combination, separation of yield changes under the historical and counterfactual distributions, measured using PNS, does not approach standard confidence levels (Supplementary Figure 6). The highest PNS of 55% is seen for positive effects of warming on Peruvian rice yields. However, although the signal of anthropogenic warming has not emerged strongly for any specific crop in any specific country, it is still possible that all 287 crop-country combinations in the sample show, in aggregate, the influence of anthropogenic warming.

In order to assess the aggregate global and multi-crop evidence for the influence of anthropogenic warming, I combine yield changes between the baseline and recent periods for all countries and crops into a single yield index. Index weighting is determined by the estimated signal-to-noise ratio of anthropogenic warming for that crop and country, in other words the magnitude of the warming signal divided by the empirical variance in the estimated signal defined using a training set of one third of the simulations (Methods). This weighting maximizes statistical power to detect the anthropogenic signal (45) since it accounts for the different response of crops to temperature change (i.e yield increases in some areas and decreases in other areas could both be consistent with the anthropogenic effect), variation in the exposure and sensitivity of crops to anthropogenic warming, and heterogeneity in the uncertainty of the estimated anthropogenic effect. The change in yield between a 1961-1970 start period and a 2008-2017 end period for each of the 287 crop-country combinations are aggregated into a one-dimensional index using this optimized weighting, shown in Supplementary Figure 7.

Figure 4a shows the distribution of this global multi-crop yield change index under historical and counterfactual forcing for the 667 simulations excluded from the training set used to estimate index weights (Methods). The distributions are reasonably well separated, with a maximum PNS of 87.4%. A test to detect the anthropogenic signal divides possible index values into two regions - those consistent and those inconsistent with the influence of anthropogenic warming – with the threshold value chosen so as to maximize statistical power (dashed line, Figure 4a). Observed values of the yield change index are well within the region of detected anthropogenic influence, consistent with historic but not counterfactual forcing. The observed yield index value of 966 falls well within the central 95% of the historical distribution, but is in the bottom 0.1% of the counterfactual distribution. Supplementary Figure 8 shows the same graph but using yield-temperature responses derived from process-based crop

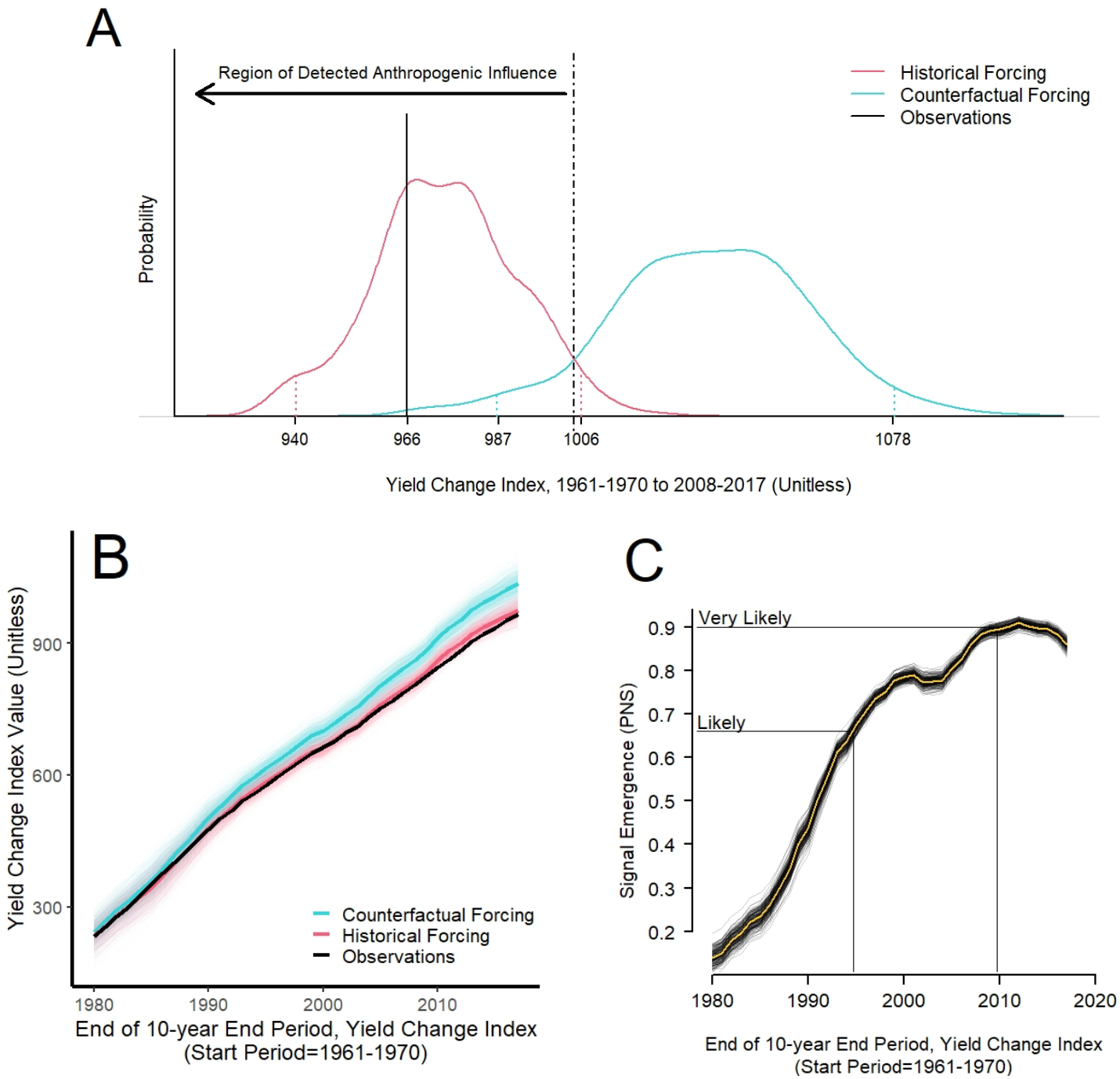

Figure Four: Identification and emergence of the signal of anthropogenic warming on global crop yields. a) Distribution of the global, multi-crop index of yield changes under historic and counterfactual forcing. Dashed line gives the threshold index value for a statistical test that maximizes the PNS. Observed values to the left of this threshold give evidence of a detected anthropogenic effect. Black line gives the observed value of the yield index, dotted lines give the quantiles defining the central 95% of the two distributions. b) Distributions of the index value over time using a rolling 10-year end-period showing the emergence of the anthropogenic warming signal. Each of the 667 simulations in the testing set of the historical and counterfactual forcing simulations is shown (thin lines) as well as the distribution means (thick lines) c) Separation of the index distributions under historical and counterfactual forcings, quantified using the PNS. Probabilities corresponding to "likely" (66%) and "very likely" (90%) are from Mastrandrea et al. (52). Black lines show variation arising from 200 draws of the training vs testing sets with the yellow line showing the median value.

models participating in the AgMIP Phase 2 experiment (39, 40), which also demonstrates both the emergence and detection of an anthropogenic warming signal on global crop yields.

Figures 4b and 4c show the emergence of this anthropogenic warming signal over the end of the 20th century by calculating the yield change index between the 1961-1970 start period and a rolling 10-year end period ending between 1980 and 2017. The index values in Figure 4b show a large secular trend in all simulations, reflecting significant gains in yield over this time period due largely to improved technology and increasing inputs. This non-stationarity even in the absence of climate change has been identified previously as a major challenge to the detection of climate change impacts in human and managed systems generally (10). However, Figure 4b also shows the gradual separation of the two distributions over time, producing the well-separated distributions shown in Figure 4a by 2017. Observed index values consistently track the historical forcing simulations. Figure 4c quantifies the time of emergence of the anthropogenic warming signal showing the increasing separation of the two distributions, measured using PNS, since the 1980s. The signal emerged strongly over the early 2000s, with PNS close to or exceeding 90% since 2010.

Figure 4a demonstrates both the emergence of the anthropogenic warming signal (through the separation of the historic and counterfactual index distributions) and the detection of a signal consistent with an anthropogenic influence in observed patterns of yield growth (through an observed index value consistent with the historic but not counterfactual distribution). However, the attribution of this detected signal uniquely to greenhouse gas emissions is a more complex question. In classic attribution studies, the spatio-temporal pattern of greenhouse gases is shown to be distinct from that of all other influences on the system (1). However, in the case of socio-economic systems such as global agriculture, this is more challenging as other system drivers such as changing technology, changing input use, and shifts in growing areas and land quality may be unobserved or poorly understood. If the effects of these drivers happen to correlate with the estimated anthropogenic warming signal, then the detected change cannot be attributed solely to anthropogenic warming.

The degree to which the detected signal can be confidently attributed to anthropogenic warming is investigated in two ways. Firstly, I test whether signal emergence and detection relies disproportionately on yield trends within a single geographic area, and therefore might be explained by idiosyncratic regional trends unassociated with warming. Supplementary Tables 1 and 2 show both the index separations (PNS values) and detection result after dropping individual crop-continent combinations, or whole continents from the aggregated index. These show that both the emergence and detection results are largely robust to the exclusion of particular regions: index separation drops from a PNS of

87.4% using the full sample to a minimum of 83.9% after dropping Asian rice. As suggested by Figure 3b, rice yield trends, because of the estimated large and non-linear effect of warming (Figure 2), are somewhat more important in the emergence result. But this is a global effect, not relying exclusively on a particular region, driven by both positive and negative effects of warming in different parts of the world.

Supplementary Figure 9 shows a second test of alternate explanations for the emergence and detection result shown in Figure 4. These figures show index separation using two alternate weighting schemes: an unweighted index (uniform weighting) and an income-weighted index. If the estimated anthropogenic warming effect is largely a result of a general, universal slowing of yield growth, which could have other explanations including slowing technological improvements or decelerating input growth, then the PNS value of the unweighted index will be similar to that of the index shown in Figure 4. Instead, the PNS of the unweighted index drops substantially from 87.4% to 62.8% (Supplementary Figure 7a), below the "likely" probability threshold of 66.67% used by the IPCC (52). Moreover, the observed index value of 203 falls within the central 95% of the counterfactual distribution, meaning the null hypothesis of no anthropogenic warming effect would not be rejected under standard confidence thresholds. Using baseline per-capita income as an index weight allows for any differential yield trends in developed vs developing countries to also affect index separation, but this has a very minor effect, increasing PNS to 64.2% compared to 62.8% for the unweighted index (Supplementary Figure 7b).

To summarize then, these supplementary analyses demonstrate that some fraction of signal emergence results from general decelerations in yield growth that the empirical yield model suggests should have accompanied anthropogenic warming in most areas (Supplementary Figure 7a). However, additional index separation required to raise the PNS from below 65% to close to 90% relies on the specific country-crop pattern associated with anthropogenic warming. This pattern arises both from the spatial variation in anthropogenic warming (Figure 1a) and the varying sensitivity of rice to warming across its range (Figure 2) and is not associated with baseline income differences across countries (Supplementary Figure 7b). Attribution of the detected pattern is therefore necessarily mixed; while a number of drivers might cause a general deceleration in yield growth, alternate explanations for the spatial pattern of yield trends (such as specific technological advances improving rice cultivation in cooler climates) are possible but less obvious.

Because the identified signal of anthropogenic warming on crops includes both reductions in wheat yields and increases in rice yields in certain areas, the net effect on caloric production is ambiguous. I therefore quantify the effect of anthropogenic warming on global food security by aggregating the

difference in agricultural production in the historic and counterfactual forcing simulations to the global level (Supplementary Figure 10a). The net effect on calorie production has been negative, dominated by wheat and maize, which are both more widely grown and more calorie dense than rice. In the 2008-2017 end-period, the central estimate is that warming from anthropogenic greenhouse gas emissions has reduced annual calorie production from wheat, rice, and maize, by 5.3%, an amount sufficient to feed 290 million people each year assuming a daily caloric requirement of 2,500 calories and allowing for 35% post-harvest losses (53). The 90% confidence interval ranges from a 12.5% loss in calorie production to a 1.9% gain.

The country-level calorie effect from anthropogenic warming is given in Supplementary Figure 10b. A consistent geographic signal is not strongly apparent due to counteracting effects from the sensitivity and exposure of crops to anthropogenic warming: rice in tropical areas is more negatively affected by warming (Figure 2) but the magnitude of anthropogenic warming is larger in temperate countries (Figure 1a). The vast majority of countries have seen net declines in calorie production. Net positive effects on are small and are limited to cooler rice-producing regions (particularly Japan and South Korea).

Comparisons to previous studies on the effects of observed climate trends over the historical record should be done with caution because of differences in the relevant time periods and forcings examined. The most direct comparison is with Lobell, Schlenker and Costa Roberts (25) who estimate that observed warming trends between 1980 and 2008 reduced maize and wheat yields by 4% and 5% respectively, with negligible net effects on rice. Here, examining the effect of anthropogenic (not observed) warming trends resulting from greenhouse gas emissions (not in combination with aerosol effects) in the 2008-2017 period, I find very similar effects on area-weighted yields for maize and wheat (5.9% and 4.9% respectively) but larger negative effects on rice (a net decline of 4.2%). The estimated net negative effect across Europe also matches previous studies connecting an observed deceleration of wheat yield growth in the region with observed climate trends (36, 37). Findings also agree with those in Ortiz-Bobea et al (54) who estimate that anthropogenic warming has depressed agricultural total factor productivity by 20%. The analysis in that paper is a ceteris-paribus one, sampling from internal climate variability and uncertainty in the TFP response to warming, but not variation in the other drivers of TFP or the residual TFP variance, as is done in this paper to demonstrate the emergence and detection of the anthropogenic warming signal.

It is important to note that the yield impacts described here are those associated with the warming effect of greenhouse gas emissions, not with the effect of greenhouse gases themselves, with

anthropogenic climate change more generally, or with all radiatively-active anthropogenic emissions. The simulations shown in Figure 4a fix rainfall at its historic value, which means that the distribution variance does not include internal variability in growing season precipitation. Adding this variation to the simulations by sampling rainfall as well as temperature from the climate model ensembles increases the distribution variance but, because there is no emergence of the anthropogenic signal in total growing season rainfall (as shown in Supplementary Figure 3), does not increase the separation of the historical and counterfactual distributions. Because of the small estimated effect of growing season rainfall on crop yields though, this effect is small. Supplementary Figure 11 shows the distribution of the historic and counterfactual yield index that includes internal variability in growing season rainfall in the distribution variance. Separation of the distributions falls slightly, from 87.4% to 84.9%.

Carbon dioxide has a directly beneficial effect on crops: a simple calculation based on a recent meta-analysis (49) suggests that CO_2 fertilization over the 1961-2017 period has raised yields of C_3 crops (rice and wheat) by 7.1% and of C_4 crops (maize) by 6.0%. These are more than enough to offset, at a global level, the negative effects of anthropogenic warming documented here. However, the effect of radiatively-active short-lived polluters such as aerosols and tropospheric ozone are also not considered. These affect crops through a number of pathways, including reducing the solar radiation available for photosynthesis, scattering incoming radiation, and direct ozone toxicity, in addition to their effects on local temperature (additional discussion in Methods) (32, 55). These effects are poorly constrained, but within certain regions, the negative effect is estimated to be much larger than benefits from CO_2 fertilization (32).

The influence of greenhouse gas emissions on the physical climate system is now well demonstrated (1, 5, 6) and a growing body of literature has documented the sensitivity of socio-economic outcomes to changes in climate (56, 57). However, directly detecting the signal of anthropogenic emissions on these outcomes is challenging because climate change may be only a small driver of change, and other key factors may be unobserved, unquantifiable, or poorly understood. Nevertheless, this analysis shows anthropogenic climate change has likely already had a discernable influence on global agricultural production, even accounting for multiple sources of uncertainty and variation. It therefore contributes to a growing literature linking climate trends to slowing productivity growth in agriculture (25, 54). It is probable that continued global warming will lead to larger effects on agriculture as well as global emergence of the anthropogenic climate change signal in other economic sectors.

Methods

A schematic illustration of the method used in this paper is given in Supplementary Figure 2. Growing season temperature change under historical forcings (40 members) and the counterfactual forcing that omits greenhouse gas emissions since 1920 (20 members) are from two large ensembles of the CESM model (38). Although many detection and attribution studies have compared the effect of historical to natural forcings, netting out the effect of aerosol cooling from greenhouse gas warming, this would greatly complicate the yield analysis. Aerosols affect crops not only via growing season temperature but also by changing the sunlight available for photosynthesis and by altering the scatter of incoming radiation (55, 58). This effect is not empirically well constrained on a global scale and varies by aerosol species (58), meaning including the aerosol effect would add substantial uncertainty to the yield response modeling. Tropospheric ozone is similarly complex in that, in addition to its effect on climate, it is also directly toxic to crops. The yield effects of ozone and aerosols through these 'non-climate' pathways is likely much larger than their effect on crops via changes in temperature (58). Accordingly this paper focuses only on the effect of radiative forcing from greenhouse gas emissions using the CESM ensembles.

Since the CESM is the only model to run these leave-one-out detection and attribution ensembles, climate model uncertainty is not sampled in the analysis. Comparisons of CESM output with historical observations across a range of climate variables suggest it is among the best-performing models within the CMIP5 ensemble (59, 60). Supplementary Figure 12a provides a comparison between observed terrestrial temperature change since 1960, the LENS distribution, and the CMIP5 inter-model spread (61). Natural variability captured by the LENS overlaps with a large majority (lower 75%) of the CMIP5 distribution. The upper 25th percentile of the CMIP5 distribution simulates rapid warming since 1990 that is outside the LENS distribution. But this upper tail is also substantially larger than warming in the observational record. Supplementary Figure 12b compares the LENS distribution to observed country-crop-level changes in growing-season temperature over growing-areas. While there is no evidence of systematic bias in the LENS warming rates, there is evidence that the range of observations is wider than captured by the LENS. This could be consistent either with noise in observational data or an under-sampling of natural variability by CESM.

Comparison to both observations and the CMIP5 distribution therefore suggests it is possible that reliance on a large ensemble from a single model may somewhat understate the true variance in temperature change, leading to overconfidence in identification of the anthropogenic signal. However, this effect is unlikely to substantively affect the main conclusions of the study for two reasons. Firstly,

the LENS distribution is missing only the highest 25th percentile of warming from the CMIP5 ensemble. This means that expanding the temperature distribution to account for the models at the high-end of the CMIP 5 distribution would likely increase the estimate of the anthropogenic warming signal, since these models appear to display a higher sensitivity to anthropogenic forcing. This would lead to a larger estimated effect on crop yields, larger signal emergence, and greater confidence in the detection result. Secondly, temperature variability is a relatively small driver of variance in the simulated index values. The distribution of index values under historical forcing using only LENS temperature variability, ignoring parameter or residual uncertainty, reduces variance by 79%, implying the empirical yield model accounts for the large majority of index variance. Therefore, it is unlikely that a small expansion of the distribution of temperature changes, consistent with observations or the CMIP5 inter-model spread, would overturn evidence for the anthropogenic signal.

National yield data for maize, wheat, and rice from 1961-2017 from the Food and Agriculture Organization (FAO) (62) is used for the empirical yield model. Although national-level FAO data are known to contain measurement error, it is the only source of global, multi-crop yield data over a time-span long enough to identify the emergence of a climate change signal. To the extent FAO yield data contains classical measurement error, for instance resulting from administrative errors in yield data collection, this will increase standard errors and residual variance, but will not bias estimates of the temperature effect on yield (63). Because both uncertainty in the yield response function and residual variance are sampled in the detection and attribution analysis, this will tend to increase the variance of the index distributions, leading to more overlap between the historical and counterfactual distributions and therefore a more conservative detection and attribution finding. If instead this error is non-classical and correlated with temperature variation then it will bias temperature coefficients in an unknown direction.

Yield data is merged with observations of temperature and precipitation from the Climate Research Unit, aggregated as described above using growing-season dates and growing areas (41, 64, 65). For winter wheat, the growing season is taken to be the four months prior to harvest date. To check robustness to alternate observational datasets, the yield model is also estimated using the Berkeley Earth temperature dataset (with CRU precipitation data) (66), and the University of Delaware temperature and rainfall datasets (67, 68). Growing area data and the calorie density of wheat, rice, and maize are also taken from the FAO (62).

An empirical model of yields is specified as follows, similar to the specification in Lobell et al. (25):

$$\log(y_{ict}) = \beta_{1c}T_{ict}I_c + \beta_{2c}{T_{ict}}^2 I_c + \beta_{3c}P_{ict}I_c + \beta_{4c}{P_{ict}}^2 I_c + \beta_{5ic}tI_{ic} + \beta_{6ic}t^2 I_{ic} + \theta_{ic} + \vartheta_{ct} + \varepsilon_{ict} \quad (1)$$

Where y_{ict} is the yield of crop c in country i in year t, $\beta_{1c}T_{ict}I_c + \beta_{2c}{T_{ict}}^2 I_c$ are crop-specific quadratics in growing-season temperature and $\beta_{3c}P_{ict}I_c + \beta_{4c}{P_{ict}}^2 I_c$ are the same in growing-season precipitation. The $\beta_{5ic}tI_{ic} + \beta_{6ic}t^2 I_{ic}$ terms are crop*country specific quadratic time trends, which capture smoothly trending, unobserved, country-crop specific factors affecting yield such as technological progress. θ_{ic} is a set of country-crop specific fixed-effect (dummy variables) capturing all time-invariant differences between crop yields and ϑ_{ct} is a set of year-crop fixed-effects capturing all changes in yield that are common across countries.

For regression stability, temperature and precipitation are normalized prior to estimation by subtracting the historical mean and dividing by the standard deviation. Climate model data is similarly transformed into common units by subtracting the same historical mean and dividing by the historical standard deviation. Only country-crop combinations with at least 15 years of data are included. This gives 355 country-crop combinations and a total of 18155 observations. Estimation is done using Ordinary Least Squares (OLS) with standard errors clustered at both the region by crop level and the region by year level. This allows for arbitrary correlation of residuals between neighboring countries and over time in the same country, as well as between different crops within the same region in the same year. The 17 geographic regions used for clustering are based on the GEO3 regions (69): Australia and New Zealand, Caribbean, Central Africa, Central Asia, Central Europe, East Africa, Eastern Europe, Meso-America, North America, NW Pacific and East Asia, South America, South Asia, South Pacific, Southeast Asia, Southern Africa, Western Africa, and Western Europe.

The regression model in total explains 92.78% of the variance in the dependent variable (R^2=0.9278). The vast majority of this explanatory power comes from non-weather terms in the model (specifically, the country-crop time trends, and the country-crop and year-crop fixed-effects). Removing the weather terms reduces model R^2 to 0.9267, meaning temperature and rainfall explain only a very small faction of residual variance in yield. However, a joint test of the 12 temperature and rainfall terms in the model clearly rejects the null hypothesis that these do not add explanatory power using both a Wald ($p<0.00001$) and a likelihood ratio test ($p<0.00001$). Supplementary Figure 13 compares the marginal temperature effect estimated in the combined regression with marginal effects from separate regressions for each region and crop. Although there is heterogeneity across regions, standard errors are large and overlapping with those from the combined model. Supplementary Figure 14 shows differences in the marginal effect of temperature estimated pre- and post-1989. Ortiz-Bobea et al (54) find evidence that the sensitivity of agricultural total factor productivity has increased over time. The same effect is not apparent for crop yields: although there is some evidence of slightly increased

sensitivity of rice yields to warming in later periods, the opposite is true of wheat and maize yields, with changes small relative to the standard error of the estimates.

Since a large part of the anthropogenic warming signal is either global or smoothly changing at the country level, this variation is captured in the year-crop fixed effects (ϑ_{ct}) and the country-crop quadratic time trends ($\beta_{5ic}tI_{ic} + \beta_{6ic}t^2I_{ic}$). Parameters of the yield-temperature response function ($\beta_{1c}T_{ict}I_c + \beta_{2c}{T_{ict}}^2I_c$) are estimated using residual variation in country-level growing-season temperature after controlling for these global changes and smooth time trends. This principally reflects inter-annual weather variability (see illustration for French wheat temperatures in Supplementary Figure 15). This residual weather variation used to estimate the response function parameters is quasi-random and therefore highly unlikely to be correlated with other factors affecting yield (70). However, non-linear panel models like that used here, which estimate heterogeneous marginal effects of warming across space, can re-introduce omitted-variable bias concerns. While country-crop fixed effects remove any effect of time-invariant omitted variables on *mean* yields, if these variables influence the temperature *sensitivity* of crops and are also correlated with average temperature, they could still bias estimated coefficients (71). Therefore, though fixed-effect models greatly alleviate concerns over omitted-variable bias, in this non-linear setting they do not completely remove them.

It is also important to note that in general, response functions estimated from non-linear panel models are a mix of short-run (without longer-run adaptations) and long-run (net of adaptation) responses (71). In a setting like this one, with large spatial relative to time series variation in the panel, a quadratic response function mostly captures the long-run response (72). That means the yield effects estimated here should be understood as net of adaptation. To the extent producers have responded to climate trends partly by investing in adaptations, those costs are additional to the yield impacts of climate trends documented here.

Supplementary Figure 4 and 8 use yield temperature responses derived from process-based crop models participating in the AgMIP Phase 2 experiment (39, 40). Methods for these findings are explained in detail in the Supplementary Information.

A distribution of 1000 possible alternate yield trajectories over the 1961-2017 period for each of the 355 country-crop combinations under both historical and counterfactual forcings is generated. These distributions reflect three sources of uncertainty: natural variability captured by the CESM ensemble, uncertainty in the parameters of the empirical yield model, and the variance in yields not explained by the yield model, captured by the residual variation. For each simulation, I first sample growing season temperatures uniformly from the historic and counterfactual ensemble, then estimate predicted yields

by combining sampled growing season temperatures with a draw from the estimated multivariate distribution of parameters of the yield model, and finally simulate yields by adding a draw from the residual distribution.

A training set of one third of the simulations (n=333) is randomly drawn from the simulations. This is used to calculate the optimal weighting of the global yield change index. Weightings in the index are given by:

$$W_{ict} = \frac{\bar{\Delta}y_{1ic} - \bar{\Delta}y_{0ic}}{Var(\Delta y_{0ic})}$$

Where $\bar{\Delta}y_{1ic}$ is the mean change in yield of crop c in country i in the historical forcing simulations between the initial 10 years of the sample (1961-1970) and the final 10 years (2008-2017) in the training set and $\bar{\Delta}y_{0ic}$ is the same for the counterfactual forcing simulations (i.e. the signal of greenhouse gas emissions on yield growth). The denominator is the estimated variance of yield changes in the counterfactual simulations. Because some countries are missing data for the start period, the number of crop-country combinations drops to 287 for this analysis.

The remaining two thirds (n=667) simulations are aggregated to a single index using the weightings derived from the training set to produce distributions of the index under historical and counterfactual forcings. The observed value of the yield index is calculated using the same weightings applied to observed yield changes. The threshold value for the index, defining the region of identified anthropogenic influence, is chosen as the value that maximizes PNS, which is the point of maximum separation of the CDF of the two distributions. For Figures 4b and 4c, the yield change index is calculated for each simulation using a rolling 10-year end period ending in each year from 1980 to 2017. Figure 4c also shows the variation resulting from sampling the training vs testing

The estimated effect of anthropogenic warming on global calorie production from wheat, rice, and maize is calculated as:

$$\Delta Cal_t = \sum_{ic} A_{ict} k_c \, \Delta\hat{y}_{ict}$$

Where A_{ict} is the area of crop c in country i in year t and k_c is the calorie density of crop c. $\Delta\hat{y}_{ict}$ is the estimated change in yield due to anthropogenic warming.

References

1. B. D. Santer, *et al.*, A Search for Human Influence on the Thermal Structure of the Atmosphere. *Nature* **382**, 39–46 (1996).

2. B. D. Santer, *et al.*, Identifying human influences on atmospheric temperature. *Proc. Natl. Acad. Sci. U. S. A.* **110**, 26–33 (2013).

3. T. P. Barnett, *et al.*, Human-induced changes in the hydrology of the western United States. *Science (80-.).* **319**, 1080–1083 (2008).

4. S. Min, X. Zhang, F. W. Zwiers, G. C. Hegerl, Human Contribution to More-Intense Precipitation Extremes. *Nature* **470**, 378–381 (2011).

5. X. Zhang, *et al.*, Detection of human influence on twentieth-century precipitation trends. *Nature* **448**, 461–5 (2007).

6. K. Marvel, C. Bonfils, Identifying External Influences on Global Precipitation. *Proc. Natl. Acad. Sci.* **110**, 19301–19306 (2013).

7. M. Dell, B. F. Jones, B. A. Olken, Temperature Shocks and Economic Growth: Evidence from the Last Half Century. *Am. Econ. J. Macroecon.* **4**, 66–95 (2012).

8. K. J. Mach, *et al.*, Climate as a risk factor for armed conflict. *Nature* **571**, 193–197 (2019).

9. O. Deschênes, M. Greenstone, Climate Change, Mortality, and Adaptation: Evidence from Annual Fluctuations in Weather in the US. *Am. Econ. J. Appl. Econ.* **3**, 152–185 (2011).

10. D. Stone, *et al.*, The challenge to detect and attribute effects of climate change on human and natural systems. *Clim. Change* **121**, 381–395 (2013).

11. W. Cramer, *et al.*, "Chapter 18: Detection and Attribution" in *Climate Change 2014: Impacts, Adaptation and Vulnerability. Working Group 2 Contribution to the IPCC 5th Assessment Report*, (Cambridge University Press, 2014).

12. D. B. Lobell, *et al.*, The Critical Role of Extreme Heat for Maize Production in the United States. *Nat. Clim. Chang.* **3**, 497–501 (2013).

13. B. Liu, *et al.*, Similar estimates of temperature impacts on global wheat yield by three independent methods. *Nat. Clim. Chang.* **6**, 1130–1136 (2016).

14. C. Zhao, *et al.*, Temperature increase reduces global yields of major crops in four independent estimates. *Proc. Natl. Acad. Sci.* **114**, 9326–9331 (2017).

15. J. R. Porter, *et al.*, "Chapter 7: Food Security and Food Production Systems" in *Climate Change 2014: Impacts, Adaptation and Vulnerability. Working Group 2 Contribution to the IPCC 5th Assessment Report*, (Cambridge University Press, 2014).

16. FAO, *Climate Change and Food Systems: Global Assessments and Implications for Food Security and Trade*, A. Elbehri, Ed. (Food and Agriculture Organization, 2015).

17. M. Lin, P. Huybers, Reckoning Wheat Yield Trends. *Environ. Res. Lett.* **7**, 024016 (2012).

18. P. Grassini, K. M. Eskridge, K. G. Cassman, Distinguishing Between Yield Advances and Yield Plateaus in Historical Crop Production Trends. *Nat. Commun.* **4**, 2918 (2013).

19. D. Ray, N. Ramankutty, N. Mueller, P. West, J. Foley, Recent patterns of crop yield growth,

stagnation, and collapse. *Nat. Commun.* **3** (2012).

20. D. B. Lobell, The Case of the Missing Wheat. *Environ. Res. Lett.* **7**, 024016 (2012).

21. A. Ortiz-Bobea, H. Wang, C. M. Carrillo, T. R. Ault, Unpacking the climatic drivers of US agricultural yields. *Environ. Res. Lett.* **14**, 064003 (2019).

22. D. B. Lobell, *et al.*, Greater sensitivity to drought accompanies maize yield increase in the U.S. Midwest. *Science* **344**, 516–9 (2014).

23. D. B. Lobell, A. Sibley, J. Ivan Ortiz-Monasterio, Extreme heat effects on wheat senescence in India. *Nat. Clim. Chang.* **2**, 186–189 (2012).

24. J. L. Hatfield, J. H. Prueger, Temperature extremes: Effect on plant growth and development. *Weather Clim. Extrem.* **10**, 4–10 (2015).

25. D. B. Lobell, W. Schlenker, J. Costa-Roberts, Climate Trends and Global Crop Production Since 1980. *Science (80-.).* **333**, 616–620 (2011).

26. E. Hawkins, R. Sutton, The Potential to Narrow Uncertainty in Regional Climate Predictions. *Bull. Am. Meteorol. Soc.* **90**, 1095–1107 (2009).

27. C. Deser, R. Knutti, S. Solomon, A. S. Phillips, Communication of the Role of Natural Variability in Future North American Climate. *Nat. Clim. Chang.* **2**, 775–780 (2012).

28. S. Sippel, N. Meinshausen, E. M. Fischer, E. Székely, R. Knutti, Climate change now detectable from any single day of weather at global scale. *Nat. Clim. Chang.* **10**, 35–41 (2020).

29. G. Hansen, D. Stone, Assessing the observed impact of anthropogenic climate change. *Nat. Clim. Chang.* **6**, 532–9 (2016).

30. I. Supit, *et al.*, Recent Changes in the Climatic Yield Potential of Various Crops in Europe. *Agric. Syst.* **103**, 683–694 (2010).

31. D. K. Ray, *et al.*, Climate change has likely already affected global food production. *PLoS One* **14**, e0217148 (2019).

32. J. Burney, V. Ramanathan, Recent climate and air pollution impacts on Indian agriculture. *Proc. Natl. Acad. Sci. U. S. A.* **111**, 16319–24 (2014).

33. F. Tao, D. Xiao, S. Zhang, Z. Zhang, R. P. Rotter, Wheat yield benefited from increases in minimum temperature in the Huang-Huai-Hai Plain of China in the past three decades. *Agric. For. Meteorol.* **239**, 1–14 (2017).

34. F. Tao, *et al.*, Historical Data Provide New Insight Into Response and Adaptation of Maize Production Systems to Climate Change/Variabilty in China. *F. Crop. Res.* **185**, 1–11 (2016).

35. T. Palosuo, *et al.*, Effects of Climate and Historical Adaptation Measures on Barley Yield Trends in Finland. *Clim. Res.* **65**, 221–236 (2015).

36. F. C. Moore, D. B. Lobell, The Fingerprint of Climate Trends on European Crop Yields. *Proc. Natl. Acad. Sci.* **11**, 2670–2675 (2015).

37. N. Brisson, *et al.*, Why are Wheat Yields Stagnating in Europe? A Comprehensive Data Analysis for France. *F. Crop. Res.* **119**, 201–212 (2010).

38. J. E. Kay, *et al.*, The Community Earth System Model (CESM) Large Ensemble Project: A

Community Resource for Studying Climate Change in the Presence of Internal Climate Variability. *Bull. Am. Meteorol. Soc.* **96**, 1333–1349 (2013).

39. J. Franke, *et al.*, The GGCMI Phase II experiment: global gridded crop model simulations under uniform changes in CO2, temperature, water, and nitrogen levels (protocol version 1.0). *Geosci. Model Dev. Discuss.*, 1–30 (2019).

40. J. A. Franke, *et al.*, The GGCMI Phase 2 emulators: Global gridded crop model simulations under uniform changes in CO2, temperature, water, and nitrogen levels (protocol version 1.0). *Geosci. Model Dev.* **13**, 2315–2336 (2020).

41. C. Monfreda, N. Ramankutty, J. A. Foley, Farming the planet: 2. Geographic distribution of crop areas, yields, physiological types, and net primary production in the year 2000. *Global Biogeochem. Cycles* **22**, n/a-n/a (2008).

42. I. Harris, T. J. Osborn, P. Jones, D. Lister, Version 4 of the CRU TS Monthly High-Resolution Gridded Multivariate Climate Dataset. *Sci. Data* **7**, 109 (2020).

43. K. E. Kunkel, *et al.*, Can CGCMs Simulate the Twentieth-Century "Warming Hole" in the Central United States? *J. Clim.* **19**, 4137–4153 (2006).

44. N. D. Mueller, *et al.*, Cooling of US Midwest summer temperature extremes from cropland intensification. *Nat. Clim. Chang.* **6**, 317–322 (2016).

45. A. Hannart, P. Naveau, Probabilities of Causation of Climate Change. *J. Clim.* **31**, 5507–5524 (2018).

46. A. Hannart, *et al.*, Causal Counterfactual Theory for the Attribution of Weather and Climate-Related Events. *Bull. Am. Meteorol. Soc.* **97**, 99–110 (2016).

47. K. A. McKinnon, C. Deser, Internal Variability and Regional Climate Trends in an Observational Large Ensemble. *J. Clim.* **31**, 6783–6802 (2018).

48. A. J. Challinor, *et al.*, A meta-analysis of crop yield under climate change and adaptation. *Nat. Clim. Chang.* **4**, 287–291 (2014).

49. F. C. Moore, U. Baldos, T. W. Hertel, D. Diaz, New Science of Climate Change Impacts on Agriculture Implies Higher Social Cost of Carbon. *Nat. Commun.* **8**, 1601 (2017).

50. W. Schlenker, D. B. Lobell, Robust negative impacts of climate change on African agriculture. *Environ. Res. Lett.* **5**, 014010 (2010).

51. W. Schlenker, D. L. Roberts, Nonlinear Temperature Effects Indicate Severe Damages to U.S. Corn Yields Under Climate Change. *Proc. Natl. Acad. Sci.* **106**, 15594–15598 (2009).

52. M. D. Mastrandrea, *et al.*, "Guidance Note for Lead Authors of the IPCC Fifth Assessment Report on the Consistent Treatment of Uncertainties" (2010).

53. P. Alexander, *et al.*, Losses, inefficiencies and waste in the global food system. *Agric. Syst.* **153**, 190 (2017).

54. A. Ortiz-Bobea, T. R. Ault, C. M. Carrillo, R. G. Chambers, D. B. Lobell, "The Historical Impact of Anthropogenic Climate Change on Global Agricultural Productivity" (2020).

55. J. Proctor, S. Hsiang, J. Burney, M. Burke, W. Schlenker, Estimating global agricultural effects of geoengineering using volcanic eruptions. *Nature* **560**, 480–483 (2018).

56. T. A. Carleton, S. M. Hsiang, Social and economic impacts of climate. *Science (80-.).* **353**, 1112 (2016).

57. M. Dell, B. F. Jones, B. A. Olken, What Do We Learn from the Weather? The New Climate-Economy Literature. *J. Econ. Lit.* (2014).

58. J. Burney, V. Ramanathan, Recent climate and air pollution impacts on Indian agriculture. *Proc. Natl. Acad. Sci. U. S. A.* **111**, 16319–24 (2014).

59. R. Knutti, D. Masson, A. Gettleman, Climate model genealogy: Generation CMIP5 and how we got there. *Geophys. Res. Lett.* **40**, 1194–1199 (2013).

60. J. T. Fasullo, Evaluating simulated climate patterns from the CMIP archives using satellite and reanalysis datasets using the Climate Model Assessment Tool (CMATv1). *Geosci. Model Dev.* **13**, 3627–3642 (2020).

61. K. E. Taylor, R. J. Stouffer, G. A. Meehl, An Overview of CMIP5 and the Experiment Design. *Bull. Am. Meteorol. Soc.* **93**, 485–498 (2012).

62. FAO, FAOSTAT, V.3 (2016) (April 4, 2016).

63. J. Angrist, J. S. Pischke, *Mostly Harmless Econometrics* (Princeton University Press, 2009).

64. I. Harris, P. D. Jones, T. J. Osborn, D. H. Lister, Updated high-resolution grids of monthly climatic observations - the CRU TS3.10 Dataset. *Int. J. Climatol.* **34**, 623–642 (2014).

65. W. J. Sacks, D. Deryng, J. A. Foley, N. Ramankutty, Crop Planting Dates: An Analysis of Global Patterns. *Glob. Ecol. Biogeogr.* **19**, 607–620 (2010).

66. BEST, Berkeley Earth Data (2018) (March 5, 2018).

67. K. Matsuura, Willmott, Terrestrial Air Temperature: 1900-2017 Gridded Monthly Time Series Version 5.01 (2018).

68. K. Matsuura, C. J. Willmott, Terrestrial Precipitation: 1900-2017 Gridded Monthly Time Series Version 5.01 (2018).

69. UNEP, *Global Environment Outlook 3: Past, Present and Future Perspectives* (Earthscan Publications, 2002).

70. O. Deschênes, M. Greenstone, The Economic Impacts of Climate Change: Evidence from Agricultural Output and Random Fluctuations in Weather. *Am. Econ. Rev.* **97**, 354–385 (2007).

71. C. D. Kolstad, F. C. Moore, Estimating the Economics Impacts of Climate Change Using Weather Observations. *Rev. Environ. Econ. Policy* **14**, 1–24 (2020).

72. P. R. Merel, M. Gammans, Climate Econometrics: Can the Panel Approach Account for Long-Run Adaptation? *Am. J. Agric. Econ.*

Acknowledgements

The work described here benefited enormously from the intellectual contribution of Alexis Hannart who developed the weighting scheme for the optimal crop yield change index. It was supported by USDA NIFA (Award # 12225279) and the Ciracy-Wantrup Postdoctoral Fellowship at the University of California Berkeley.